Geomorphology 389 (2021) 107841

Contents lists available at ScienceDirect

Geomorphology

journal homepage: www.elsevier.com/locate/geomorph

Assessing geomorphic floodplain models for large scale coarse resolution 2D flood modelling in data scarce regions

Francisco Peña [a,b,c,d,e,*], Fernando Nardi [a,c], Assefa Melesse [d], Jayantha Obeysekera [e]

[a] WARREDOC, University for Foreigners of Perugia, Perugia, Italy
[b] Department of Civil and Environmental Engineering (DICEA), University of Florence, Florence, Italy
[c] Institute of Environment (InWE), Florida International University, Miami, FL, USA
[d] Department of Earth and Environment, Florida International University, Miami, FL, USA
[e] Sea Level Solutions Center, Florida International University, Miami, FL, USA

ARTICLE INFO

Article history:
Received 14 August 2020
Received in revised form 3 June 2021
Accepted 22 June 2021
Available online 25 June 2021

Keywords:
DEM
Geomorphological relationships
Hydraulic geometry
Coarser resolution 2D hydraulic modelling

ABSTRACT

River valleys are dynamic living ecosystems of utmost importance for flood attenuation that are shaped by inundation dynamics. Topographic and bathymetric surveys represent pivotal information for accurate and up-to-date floodplain studies. Both floodplain morphology as well as fluvial river cross section and thalweg profiles are required for inundation modelling and mapping. However, economic and technical limitations hinder their availability in some regions, resulting in challenges to build two dimensional (2D) flood wave routing simulations at proper accuracy and resolution. In this study, we assess the effectiveness of characterizing the fluvial morphology by means of geomorphic methods (GMs). Different GMs, used as surrogates of fluvial bathymetry, are tested and compared to a dataset of surveyed natural cross sections available for the Tiber River basin (Italy). Quantitative flood modelling performances are developed using a validated 150 m flood model, providing inundation extent and floodplain flow depths for the 200 years return period event. The ability (or inefficiency) of surrogating the lack of surveyed fluvial bathymetric data with GMs for supporting large scale hydraulic inundation modelling studies is assessed by testing the following 5 floodplain modelling configurations: (1) rectangular shaped cross section; (2) floodplain-based; (3) global river database; (4) linear regression bathymetric relationship; and (5) and a very coarse 700 grid resolution. In addition, two Global Flood Hazard Mapping (GFHM) products (hydrological, and hydrogeomorphic) were used as part of the large scale floodplain modelling evaluation framework. Results demonstrate that, once the fluvial channel flow area is preserved, all tested GM models produce consistent simulation of inundation depths and extents (Fit index ≥ 0.90). This work provides a quantitative assessment of the validity of the hypothesis stressing that the floodplain conveyance capacity is the driving principle of flood inundation dynamics under extreme flooding scenarios. Understanding the role of geomorphology during extreme magnitude floods may support the idea that under specific conditions, high resolution models and detailed topography/bathymetry are surplus to requirements. This work supports the application of geomorphic approaches over large riparian domains as a parsimonious solution for flood hazard mapping in data scarce regions for applications beyond flood mitigation and forecasting.

1. Introduction

Floodplains are dynamic ecosystems that play a crucial role in the natural process and ecological balance of fluvial environments, along with providing beneficial function, resources and advantages to society (Nardi et al., 2006, 2018a). Historically, river-floodplain landscapes have been influenced by anthropogenic processes. As a result, the continuous changes in land-use triggered the encroachment of river corridors and low-lying valleys to favor urbanization, population growth and economic development challenge the capacity of floodplains to store flood waters in undisturbed natural areas, ultimately increasing river flood risk (Burby, 2006; Di Baldassarre et al., 2018). Riverine flooding – generally caused by extreme precipitation events – is among the most common natural hazard worldwide (Alfieri et al., 2017; IPCC, 2014; UNISDR, 2015) causing devastation and major social, economic and environmental impacts (Doocy et al., 2013; Gan et al., 2012; Montanari, 2012). Flood risk maps serve to identify flood-prone areas and are necessary for numerous applications, including land-use planning, floodplain zoning, environmental protection, insurance premiums, decision making, policy development and hazard mitigation strategies (Annis et al., 2020b; Convertino et al., 2019; Ignacio et al., 2015; Löwe et al., 2017; Marco, 1994).

Recent technological and scientific advancements exponentially increased the robustness of numerical algorithms and methods to

* Corresponding author at: WARREDOC, University for Foreigners of Perugia, Perugia, Italy.
E-mail addresses: fpena023@fiu.edu, francisco.pena@unistrapg.it (F. Peña).

https://doi.org/10.1016/j.geomorph.2021.107841
0169-555X/

fathom the severity of varying flood scenarios in river basins, improving the ability to predict inundation patterns at different scales (Annis et al., 2020a; Annis and Nardi, 2019; Bierkens, 2015; Papaioannou et al., 2016; Saksena et al., 2019; Saksena and Merwade, 2017; Sampson et al., 2012). Physically-based hydrodynamic models are subject to defined input data, such as the floodplain elevations, hydraulic geometry, hydrologic regimes, and surface roughness to simulate inundation depth and extent. For instance, topography is recognized as the governing factor and main input for hydraulic modelling (Farr et al., 2007), playing a crucial role in floodplain inundation dynamics (Maidment and Djokic, 2000). Remote sensing technologies are constantly improving the quality and availability of digital terrain models (DTMs), increasing the precision of land surface elevations. Nowadays, a number of official national and international organization repositories offer available open-access topographic datasets for academic and professional purposes. In this regard, scientists and experts have benefited from the use of Shuttle Radar Topography Missions (SRTM) DTMs, coupled with hydrological datasets to develop hydraulic and hydrogeomorphic Global Flood Hazard Models (GFHM) at high resolutions (Dottori et al., 2018; Nardi et al., 2019; Ward et al., 2015).

Conversely, river bathymetry remains prohibitive in most regions due to surveying costs, time constraints, and the challenging distributed parameterization, often undermining its applicability in large reaches (Domeneghetti, 2016). Specialized remote sensing methods, in the form of multibeam sonar surveys (Altenau et al., 2017) or unmanned aerial systems (UAS) (Manfreda et al., 2018), have revolutionized the acquisition of underwater river bathymetry as well as monitoring changes in bed topography compared to traditional in-situ measurements (Barnard et al., 2011; Cobby et al., 2001; Hilldale and Raff, 2008), with their accuracy subject to environmental factors and technical limitations (Kasvi et al., 2019). In the same manner, the parameterization of empirical equations has been used as a parsimonious alternative to infer river geometry and related hydrologic variables (e.g., rating curve, discharge) from available observations (e.g., water widths) (Dodov and Foufoula-Georgiou, 2004), and has been applied in numerous geographical and climate settings with reasonable accuracy (Hey and Thorne, 1986; Knighton, 1975; Lewis, 1969; Miller, 1958). The well-known and largely explored Leopold and Maddock (1953) power laws are used for developing large-scale fluvial geomorphologic relationships by means of hydraulic geometry relationships (width, depth, and flow area).

Although high-resolution data and models are a rising trend in the flood modelling community to account for the effects of urban infrastructure and floodplain features on flood wave propagation (Dottori et al., 2013; Wing et al., 2017), coarser resolution flood models also offer multiple advantages. Coarse flood modelling support parsimonious simulation efficiency and consistent predictions characterized by good levels of accuracy, especially when precise water surface/dynamics simulations are not mandatory. For example, coarser resolution models may be suited to simulate extreme flood events over a large-scale riparian ecosystem for land zoning or socio-demographic studies. Several studies have analyzed the effects of fluvial terrain processing methods in coarser domains with better performance metrics under high return periods (Cook and Merwade, 2009; Saksena et al., 2020; Saksena and Merwade, 2015). In this case, the discharge volume dictates the flood inundation extent, while the vertical ground elevation, channel bed accuracy and mesh resolution assume a secondary role (Savage et al., 2016).

Furthermore, the combined knowledge of geomorphic and hydrologic science innovations fostered flood hazard models from regional to global scales (Bates, 2012; Di Baldassarre et al., 2011; Schumann et al., 2018). GFHM use different means for representing river channel networks and geometry including hydrographic datasets (Andreadis et al., 2013; Lehner et al., 2008; Yamazaki et al., 2014), mathematical algorithms (Nardi et al., 2019; Neal et al., 2012; Pappenberger et al., 2012; Sampson et al., 2015), or by integrating climatic models (Winsemius et al., 2013). The applicability of large-scale and high-resolution models in real-time flood emergency operations and early warning systems has been the preferred method for data-rich locations, remaining disclosed to most regions due to the considerable computational expense (Leskens et al., 2014). As a result, alternative methods such as pre-simulated flood catalogues have been used as a simplified low-cost option to expand inundation forecasts across regions (Bhola et al., 2018; Dottori et al., 2017; Henonin et al., 2013). Nevertheless, most remote data-scarce locations may have restricted access and usability of scenario-based flood products from static hydraulic results. In contrast, large-scale coarser 2D flood models, under specific conditions, are capable to provide reasonable fast inundation simulations of flood physics based on parsimonious hydraulic models at the cost of topographic and hydro-modelling inaccuracies without the need to prepare any simulation beforehand.

Therefore, the choice of spatial resolution and bathymetric data is an important aspect to consider by flood modelers (Dey et al., 2019; Savage et al., 2016), as an adequate balance between the model's complexity and detail are critical for the model output and performance metrics (Dottori et al., 2013; Hunter et al., 2007). Studies on the characterization of river geometries through simplified cross sections have mainly focused on flood level prediction at different scales (Gichamo et al., 2012; Glenn et al., 2016; Grimaldi et al., 2018; Neal et al., 2015; Trigg et al., 2009). As in Grimaldi et al. (2018), this research focus on the importance of matching the channel flow area and proper floodplain resolution. The rationale behind this work is that geomorphic parameters may be constrained to have a good approximation of the channel conveyance capacity, specifically to provide timely flood hazard predictions when the floodplain act as a major water storage unit due to channel overbank flow (Valentová et al., 2010).

Although large-scale flood models are valuable tools for interdisciplinary research to assess economic impacts (Jonkman et al., 2008), sociodemographic patterns (e.g., migration, displacement risk, social vulnerability) (Kam et al., 2021; Scott et al., 2019; Twilley et al., 2016; Wing et al., 2020), and environmental management, most flood hazard products are determined by fixed return periods, which neglect the floodplain inundation dynamics. Coarse resolution flood models may support novel discovery on effective multiple scenario evacuation studies or decision making where it is important to simulate the propagation of fluvial flood wave dynamics, wave progression, velocity, impact force and residence times at minimum computational costs. For instance, agricultural management is likely to benefit from coarser 2D flood models as current crop flood damage assessments are predominantly based on floodplain zoning, remote sensing, and satellite-derived statistics (Chau et al., 2013; Di et al., 2017; Tapia-Silva et al., 2011), with a limited number of local studies where flood physics are preserved (Pistrika, 2010; Veja-Serratos et al., 2018; Vozinaki et al., 2015).

In this paper, we elaborate on the value of geomorphology as a key driver of flood risk by investigating the potential of geomorphic laws approaches in a 2D coarser-resolution hydraulic model. We argue that the carrying capacity (e.g., channel flow area) of floodplains is the driving principle in floodplain inundation models for extreme return period events (e.g., rare floods when the channel conveyance is orders of magnitude less than the flood volume), and the representation of the channel geometry and DEM uncertainties are not as important to derive accurate inundation extents (Bhowmik and Stall, 1979; Bhuyian et al., 2015; Mejia and Reed, 2011). A validated flood hazard model built using surveyed natural cross sections is used to compare the inundation extent and depth of proposed geomorphic methods, as well as two GFHM paradigms (hydrogeomorphic, and hydraulic mapping products respectively) (Di Baldassarre et al., 2020). A quantitative assessment, in terms of computational and spatial metrics of the study area, is presented to assess the level of uncertainties and performance at low computational costs.

2. Data and methods

2.1. Study area

The Tiber River basin is the second largest river basin in Italy, with a catchment area of 17,800 km^2, and the third in terms of discharge after the Po and Adige. The basin originates from the Italian Apennines in Emilia-Romagna and discharges into the Tyrrhenian Sea, with a total length of 405 km (Fig. 1). The selected river sub-catchment starts at the Umbria-Lazio regional boundary just downstream of the city of Orte (12°23′ E–42°27′ N) and ends upstream of the urban area of Rome, where the Castel Giubileo dam is located (12°29′ E–41°59′ N). This river segment is named "Tiber middle valley" for its position downstream of the upper basin and the coastal area. The river is historically an area of hydrological related disasters, specifically floods and landslides (Reichenbach et al., 1998). According to the flood risk

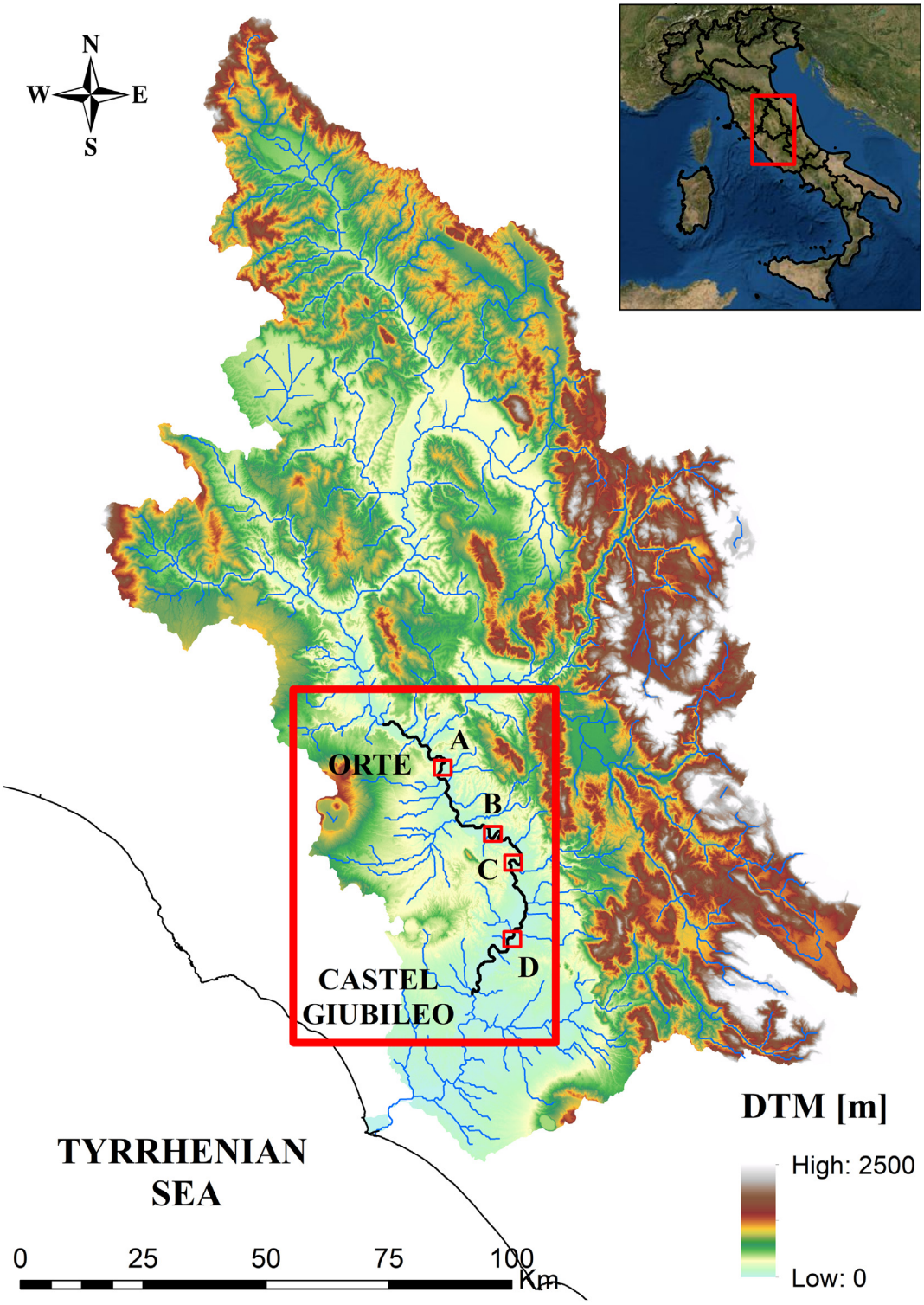

Fig. 1. Location map of the Tiber River basin in central Italy and the study area represented by the red square. The stars indicate the Tiber river reach (black line) considered for the implementation of the hydraulic model. The schematized river cross sections (A, B, C, and D) are presented in Fig. 2.

management plan issued by the Tiber River Basin Authority (TRBA, 2010), the river maximum conveyance capacity of Tiber middle valley is approximately 900 m^3/s, which is often exceeded, also in occasion of frequent floods. Frequent flooding events usually reach discharges higher than 2000 m^3/s, causing channel overbank flow and inundation along the floodplain extent, as happened recently during 2008, 2010, 2012 and 2015 events. Although agricultural and forestlands mostly cover this area, urban settlements and infrastructure have been severely affected by floods over the past 20 years (Manfreda et al., 2014; Tauro et al., 2016).

2.2. Data

Data sets required to build the 2D hydraulic model consist of topographic and hydrologic data as well as geospatial data and aerial imagery to define land use properties. This study uses a LIDAR aerial survey produced by the Italian Ministry of Environment National Cartographic Portal (PCN). The available LIDAR dataset comprises a 1 m resolution Digital Elevation Model (DEM). To build the floodplain topography of the entire study domain, the LIDAR DEM served to produce a Digital Terrain Model (DTM) of the study domain at 5 m resolution. The Tiber River Basin Authority provided a bathymetric survey of the entire floodplain domain and a calibrated 1D HEC-RAS model, consisting of 92 fluvial cross sections uniformly distributed in the 120 km river reach. Similarly, the TRBA flood risk management plan produced the hydrology using real events and synthetic case scenarios with different return periods. A hydrologic input of a 200-year return period hydrograph designed for the area of study was selected for this study. The use of aerial imagery helps to trace the channel domain and characterize the top width during the model buildup process in the digital grid domain. Furthermore, a 2D hydraulic model at 50 m resolution gathered from the TRBA served as a benchmark model to assess the calibration and validation input topographic data, land use/land cover, soil type information, roughness coefficients, rating curves, infrastructure and hydraulic features that represent the area of study. The latter is used for calibration and validation purposes of the developed models presented in the next section.

In terms of GFHM, two global flood mapping datasets served to compare the flood inundation levels and extend to the benchmark reference model for a return period of 200 years. The first dataset is the hydraulic flood hazard map for Europe developed by the Joint Research Center (JRC) (Dottori et al., 2016) at 100 m resolution. It is based on streamflow data and is computed using hydrodynamic simulations. The second is a global hydrogeomorphic mapping product (GFPLAIN250m) (Annis et al., 2019; Nardi et al., 2019) that delineates the Earth's floodplains and landscape features on a 250 m model resolution (Table 1).

2.3. Hydraulic model: FLO-2D

FLO-2D is a hydraulic model used for simulating rainfall-runoff, flood wave and debris flow routing processed for modelling and mapping watershed, riverine, urban, and coastal floods. The model is a quasi-2D hydraulic model, physically grid-based, that solves the differential form of the continuity [Eq. (1)] and momentum equations [Eq. (2)] through a simple volume conservation approach (O'Brien et al., 1993).

$$\frac{\partial h}{\partial t} + \frac{\partial hV}{\partial x} = i \tag{1}$$

$$Sf = So - \frac{\partial h}{\partial x} - \frac{V}{g} \cdot \frac{\partial V}{\partial x} - \frac{1}{g} \cdot \frac{\partial V}{\partial t} \tag{2}$$

where h is the flow depth, V is the depth-averaged velocity in one of the eight flow directions x. t is the time variable and i the excess rainfall intensity (if applied). The momentum equation is based on the Manning equation and is the relationship of bed slope (So), the pressure gradient ($\partial h/\partial x$), and the convective ($V\partial V/g\partial x$) and local acceleration ($\partial V/g\partial t$). The abovementioned equations represent the 1D depth-averaged channel flow. The full dynamic flow connectivity between 1D channel overbank flow and 2D floodplain topography comes from the fusion of the channel feature carved into the floodplain topography, and the full dynamic wave momentum equation is only applied when the channel conveyance capacity its exceeded, limited by the volume in the channel (i.e. Quasi-2D). Topography and flow resistance (Manning values) determine the channel-floodplain interactions and flow propagation dynamics in eight potential direction flow paths, the four cardinal (N, S, E, and W) and four ordinal (NE, SE, NW, and SW) through the squared grid elements.

Similarly, urban features (such as buildings, streets, and levees), physical processes, and conveyance structures can modify the flow distribution in the domain. FLO-2D finite difference numerical scheme verifies the numerical stability criteria is satisfied every time step in each grid element to preserve the continuity of flood volume in the domain for the specified simulation time. The channel bathymetry can be represented with surveyed or synthetic shape cross sections data. The Grid Developer System (GDS) supports the FLO-2D system on preparing the input data files required to run a simulation, including the DTM, boundary conditions (hydrologic data as inflow, and outflow elements), channel geometry, and physical obstructions that influence changes in the flow direction (levees, buildings, bridges, hydraulic structures, etc.). See O'Brien et al. (1993) for a complete description of the model.

2.4. Topography

The selected hydraulic model, FLO-2D, requires a discretized system of square tiles to represent the topography of the floodplain domain. The grid size of the computation domain defines the model resolution. The FLO-2D GDS PRO interface gathers as input a 5 m resolution DTM to create the interpolated topographic surface by means of the nearest neighbor interpolation method (ESRI, 2011; Grimaldi et al., 2004, 2005; Sibson, 1981).

The bare earth model DEM produced from LIDAR in FLO-2D is free from natural and urban features (e.g., buildings, levees, bridges) to preserve the original topography of the area. Nevertheless, these structural

Table 1
Datasets description and sources.

Name	Data format/software	Data content	Source
LIDAR DEM	ASCII grid	Digital terrain model for the entire domain	Italian Ministry of Environment National Cartographic Portal (PCN)
Surveyed cross sections	Shapefile + HEC-RAS model	92 fluvial cross sections to build a 1D HEC-RAS model	Tiber River Basin Authority (TRBA)
Hydrology	Text file	200-year return period from upstream node (Orte)	Tiber River Basin Authority (TRBA)
Aerial imagery	TIFF file	Aerial imagery for the entire river domain	PCN and TRBA
Flood model	FLO-2D	50 m resolution model for the entire domain	TRBA
Hydraulic mapping	Raster	Flood map at 100 m resolution for a 200-year return period	Flood hazard maps at European and global scale by the Joint Research Center) (Dottori et al., 2016)
Hydrogeomorphic mapping	Raster	Floodplains topography based map at 250 m resolution	Global high-resolution dataset of Earth's floodplains (GFPLAIN250m) (Nardi et al., 2019)

features were inserted into the model as area and width reduction factors to account loss of storage and redirection of flow dynamics in the topographic based model (O'Brien, 2011).

While the application of fluvial terrain processing approaches in large scale domains has been done in the past, coarser resolutions can clearly impact the accuracy of the floodplain terrain and river cross sections. Coarser resolution influence the position and elevation of river banks and thalweg profile, resulting in biased data and errors in the hydraulic conveyance capacity (Bhuyian et al., 2015; Biancamaria et al., 2009; Brandt, 2005; Jung et al., 2010; da Paz et al., 2011; Saksena and Merwade, 2015).

This work adopts the methodology developed by Peña and Nardi (2018) for upscaling topographic data resolution from a validated 50 m grid model. The channel bathymetry was surrogated to synthetic channel cross-sections and the floodplain DTM was resampled to coarser resolutions using the same interpolation method while preserving the channel thalweg and conveyance capacity, producing consistent inundation results.

Fig. 2 shows the topographic plan view of selected floodplain cross section segments derived from the high resolution 5 m DEM to produce a 50 m, 150 m and 400 m grid resolution, respectively. It can be noted that the approximation and loss of topographic information in coarser

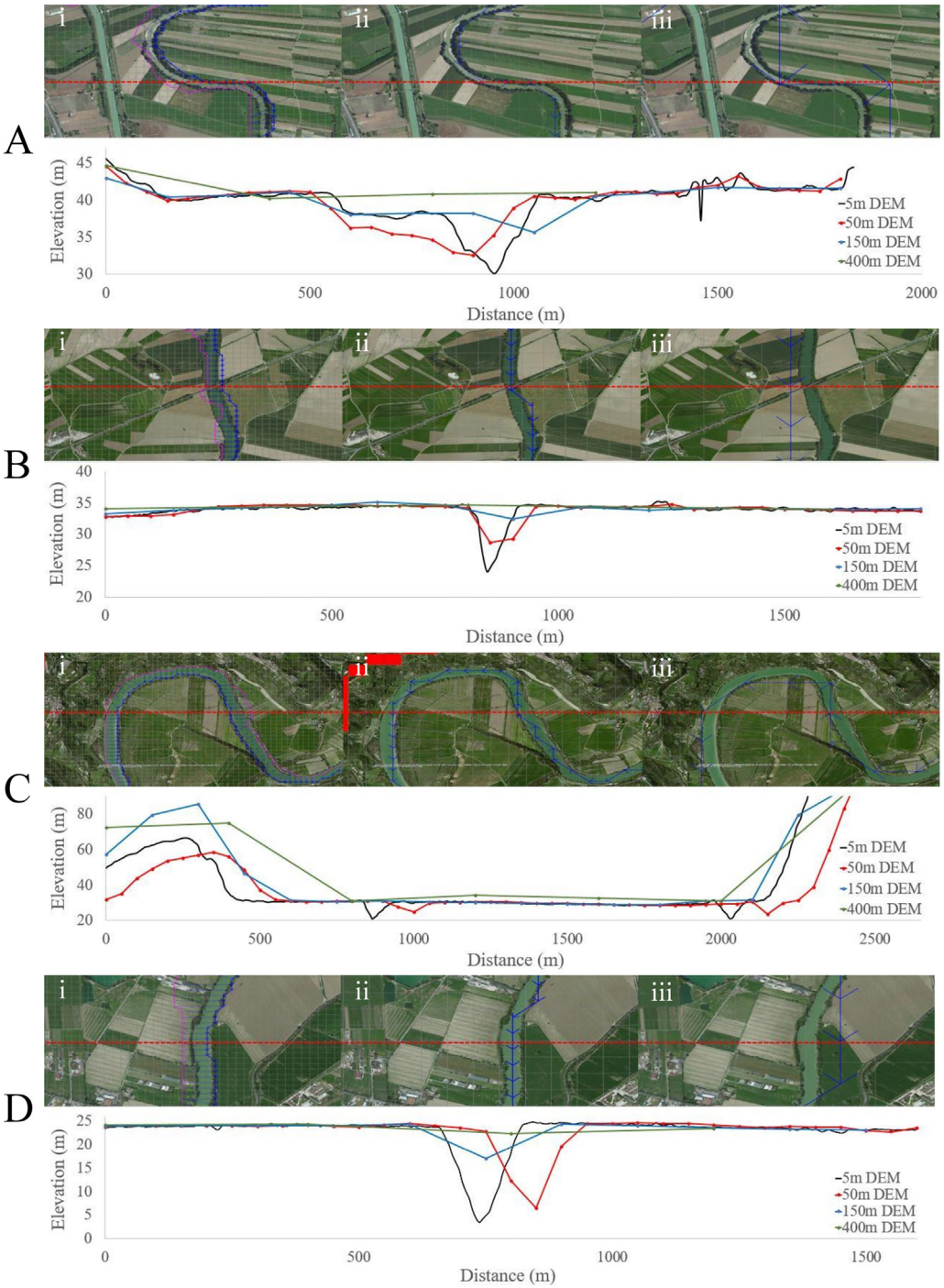

Fig. 2. Four sample locations (Fig. 1) are analyzed to test the impact of cross section geometry using varying resolutions in the computational domain. The 5 m floodplain terrain model cross section (black) is compared to interpolated 50 m (i = red), 150 m (ii = blue), and 400 m (iii = green) resolution DTMs. The upper and bottom plots show, respectively, the horizontal and vertical displacement of the interpolated floodplain grid schematization and cross section as respect to the high resolution DTM.

resolutions misrepresent the surveyed 5 m DTM, as the accurate representation of the cross section is a function of the model grid resolution. Nevertheless, the differences in the channel and floodplain conveyance capacities does not suggest a direct implication that flood modelling inaccuracies are on the same order of magnitude.

2.5. Hydrology

The design hydrology for this study was gathered from the TRBA flood frequency analysis studies. The 200-year hydrograph, with a peak discharge of 3600 m^3/s, is used as hydrologic forcing for the hydraulic model. The hydrograph base time, including rising and recession limb, determine a total simulation time of 350 h. The designed trapezoidal shape hydrograph consists of a steep increase in flow at the beginning, reaching the peak discharge, and a continuous decrease rate with uniform flow volume (Fig. 3). Positively skewed hydrographs are characterized by their steeper rising limb compared to the recession limb (Dingman, 2009). The trapezoidal hydrograph attempts to replicate the basin runoff dynamics at the upstream basin inlet (Orte), by considering enough flood volume distributed over a certain amount of time to trigger floodplain inundation.

2.6. Model configuration and set-up

Boundary conditions are characterized by the hydrologic forcing. The design hydrograph corresponds to a return period of 200 year at the upstream of the study domain, while the downstream boundary condition is set to allow the flood flows to exit the computational domain in undisturbed uniform flow conditions. For simplicity, the channel roughness coefficient were assumed constant (0.04), while the Manning values distributed throughout the floodplain are assigned based on the land use data.

The simulations were performed using a regular laptop machine, a single core Intel® Core™ i7-5500U CPU @ 2.40 GHz, 2401 MHz processor with 8.0 GB of memory (RAM).

2.7. Fit index analysis

The F-index [Eq. (3)] is a spatial performance measure method that compares reference and predicted model results for flood inundation modelling studies (Aronica et al., 2002; Bates et al., 2005; Bates and De Roo, 2000; Nardi et al., 2018b):

$$F = \frac{A_{ref} \cap A_{mod}}{A_{ref} \cup A_{mod}} \tag{3}$$

where $A_{ref} \cap A_{mod}$ represents the intersection of pixels between inundated and predicted model results and $A_{ref} \cup A_{mod}$. Value performance can range from excellent (F = 1), when perfect overlapping between reference and predicted areas is achieved, or poor (F = 0) when no agreement exists between flood areas.

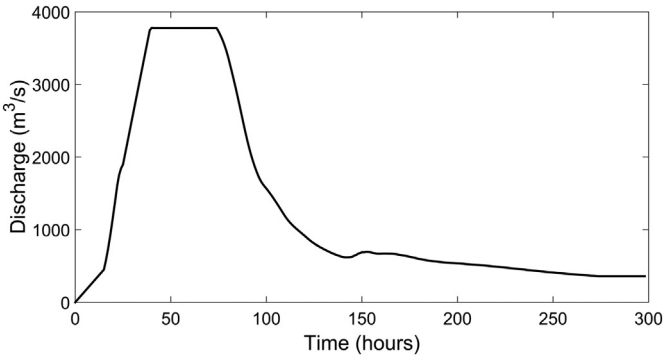

Fig. 3. Simulated 200 year designed input hydrograph for the Tiber River.

3. Procedure

In this section, we intend to assess the potential of geomorphological approaches in a defined 2D hydraulic modelling framework by replicating the methodology of Peña and Nardi (2018). The goal is to apply varying fluvial bathymetric configurations (channel flow area, top width, and maximum depth) in coarser resolutions and compare the simulated inundation depth and extent. The choice of a 150 m and 700 m resolutions was motivated by testing quantitative goodness of fit estimates and computational efficiency, thus following standard flood modelling practices is beyond the scope of this study. The first test aims to create synthetic rectangular channel cross sections by preserving the reference model channel depth, flow area, and thalweg profile. Second, spatial analysis skills supported the extraction of the lowest 5 m LIDAR DTM elevations of each cell within the river domain, creating a pure topographic-based model without a channel feature. Third, a simple global river bankfull width and depth database served to create the channel geometry. Fourth, the channel is generated by using hydraulic geometry relationships of existing data, and ultimately, upscaling the 2D floodplain terrain model to produce a 700 m coarser resolution. Moreover, two Global Flood Hazard Mapping (GFHM) products (hydrological and hydrogeomorphic) were used as part of the large-scale floodplain modelling evaluation framework All presented tests evaluate the differences in the hydraulic modelling results.

The implemented procedure was based on the following four steps:

(i) Building the 2D flood reference model at 150 m resolution

Natural cross section model (GM1): The reference river-floodplain inundation model was set in a 150 m grid resolution. The channel bathymetry was based on 92-surveyed cross sections from an existing HEC-RAS model. The channel profile was created by assigning the individual surveyed cross section data to the overlaying cells. To obtain the entire hydraulic characteristics of the channel (width, depth, slope, etc.), the cross sections were interpolated across the complete channel, producing 712 cells in the river domain for which the channel top width, maximum depth and flow area were determined. This model has an accurate representation of the flood depth and extent compared to the reference validated 50 m resolution model gathered from TRBA.

(ii) Interpolation of natural cross sections to produce a synthetic rectangular channel bathymetric model preserving channel flow area

Synthetic cross section (GM2): This configuration was built on the reference model, with the same resolution (150 m), by substituting the natural cross sections with synthetic rectangular cross sections. The rectangular shape height was constrained to the floodplain surface and to the reference thalweg profile, while the width varied to preserve the flow area. The hypothesis here was to define a rectangle that best approximates the surveyed cross section, giving priority to the conservation of the channel slope (i.e., thalweg profile) and conveyance (i.e., flow area). The top width was used as calibration parameter in this channel bathymetry interpolation.

(iii) Use of geomorphic approaches

Floodplain unconfined model (GM3): The 1D river channel feature and related channel flood wave routing process were not considered in this model. The high resolution 5 m DTM acted as input terrain data to assign the lowest topographic elevation to each of the former channel cells. The input flow hydrograph was assigned to the same upstream location and the unconfined overland flow propagation was simulated

throughout the floodplain domain, omitting the channel routing and channel-floodplain flow exchange processes.

Global river database (GM4): This approach applied a simple near-global dataset of bankfull widths and depths of rivers (Andreadis et al., 2013) with confidence intervals based on the HydroSHEDS (**Hydro**logical data and maps based on **SH**uttle **E**levation **D**erivatives at multiple **S**cales) hydrography data and the hydraulic geometry equation by Moody and Troutman (2002) [Eq. (4)]:

$$\text{Width} \propto 7.2Q^{0.5}; \text{Depth} \propto 0.27Q^{0.3} \quad (4)$$

where Q is in m^3/s, and width and depth are in m. The application of geomorphic power-law relationships for river width, depth, and velocity (Leopold and Maddock, 1953) with historical streamflow data proved key in the development of regionalized regression equations to produce global estimates of river geometry. Here we extracted from the database the river widths and depths at 95% confidence intervals to create a synthetic rectangular cross-section.

Geomorphic power law (GM5): A regression curve was used for interpolating data from the reference bathymetric model. This procedure relied on the use of recent aerial imagery to measure the channel width at the locations associated to the surveyed river cross sections. A power regression formula ($d = 0.8885w^{0.5345}$) was adopted to calculate the river depth d as a function of the channel top width w.

Coarser resolution model (GM6): The GM1 model was upscaled to a 700 m resolution. This high resolution 5 m DTM terrain data was used as input to interpolate the topography to a coarser grid size. The surveyed channel cells were identified in the new coarser grid and assigned to their respective channel grid cell. This method was developed analogously to GM2, which aimed to preserve the bathymetric characteristics of flow area, and channel thalweg by using a rectangular channel shape model, but at very coarse resolution. This test was already performed by Peña and Nardi (2018).

(iv) Inundation model runs and postprocessing of simulated water surface simulations

The simulated water surface of all models was intersected with a 30 m resolution DTM to produce the final inundation extent and flood depths. The post-processing of downscaling coarser resolution allowed a sharp display of the real flooding conditions, compared to coarser grid cells that would not provide additional value to the modelling results. Fig. 4 provides a schematic representation of the proposed procedure.

Regarding the global flood hazard mapping products (GFHM), we compared two GFHM methodologies with the benchmark reference model (GM1) to assess the flood inundation levels and extent. The hydraulic flood hazard map for Europe (Dottori et al., 2016) is a product developed by the Joint Research Center (JRC) at 100 m resolution for different return periods (100, 200 and 500 years) that is based on streamflow data and is computed using hydrodynamic simulations. This model uses daily river discharges from the Global Flood Awareness System (GloFAS) (Alfieri et al., 2014) as input for two-dimensional hydrodynamic models at local scales at 100 m spatial resolutions. The Global hydrogeomorphic mapping product (GFPLAIN250m) (Annis et al., 2019; Nardi et al., 2019) based on Earth's floodplains and landscape features, implements a methodology that is able to delineate the floodplain extension of valleys through geomorphic algorithms at 250 m resolution, with the goal to capture the full spatial extension of fluvial flooding dynamics.

4. Results

The outcomes produced by the six geomorphic methods and comparison with the GFHM are presented in this section to evaluate the role of channel geometry in terms of the simulated water surface elevation profile and flood extent for a return period of 200 years. Fig. 5 depicts the channel characteristics of each GM approach. The outcomes suggest that the channel bed elevation and flow area are only preserved in models derived from natural and synthetic cross sections (GM1, GM2, and GM6). GM4 and GM5 are based on a global database and scaling relationship, respectively, while GM3 is omitted from the channel dimension analysis because the channel feature is not considered in the model.

Fig. 6 represents the simulated flood profile along the river channel of the six geometric approaches. Changes in the channel cross-section geometry, slope, bed elevation, and resolution can result in variations (overestimation, or underestimation) of the water surface elevation (WSE) and river discharge (Fig. 6). For example, the geomorphic methods derived from the floodplain terrain analysis (GM1, and GM2), and coarser resolution (GM6) have consistent behavior along with the channel profile and bed profile. On the same note, GM5 applies a power regression formula derived from the reference GM1 model to calculate the channel depth results in similar WSE. GM3 uses the minimum floodplain elevation of the channel grid location as thalweg, which follows a similar path, with only minor differences in steep gradient changes. Conversely, GM4 has a higher thalweg profile elevation compared to other approaches, clearly overestimating the WSE of the channel.

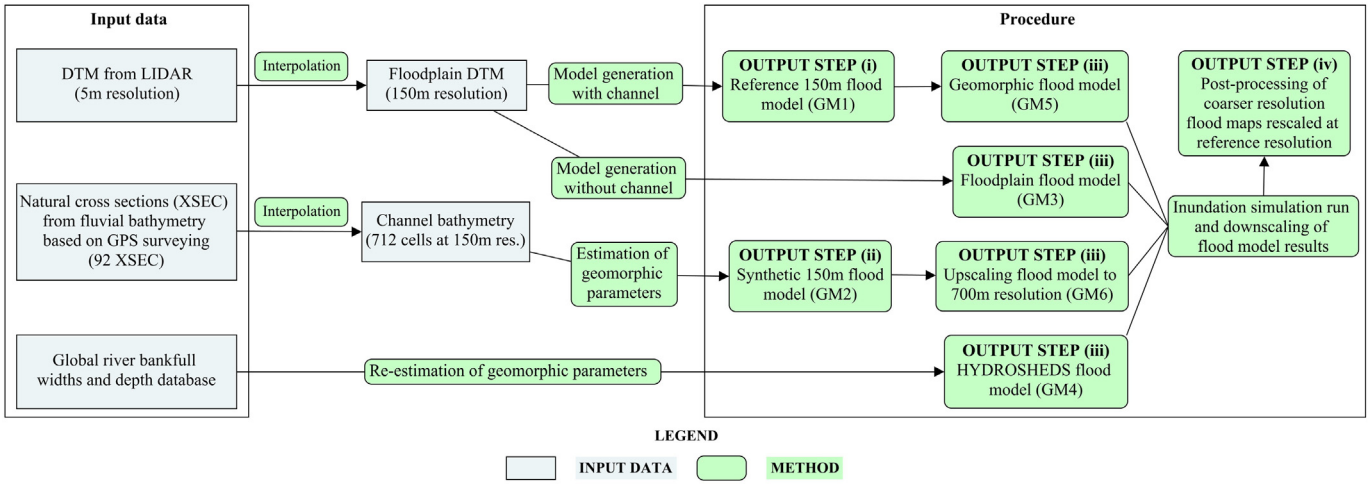

Fig. 4. Flow chart describing the procedure implemented for the application of different geomorphic models, including the use of natural and synthetic fluvial bathymetry (GM1 and GM2), floodplain unconfined model (GM3), global river database (GM4), geomorphic power law approach (GM5), and resampling floodplain terrain data (GM6).

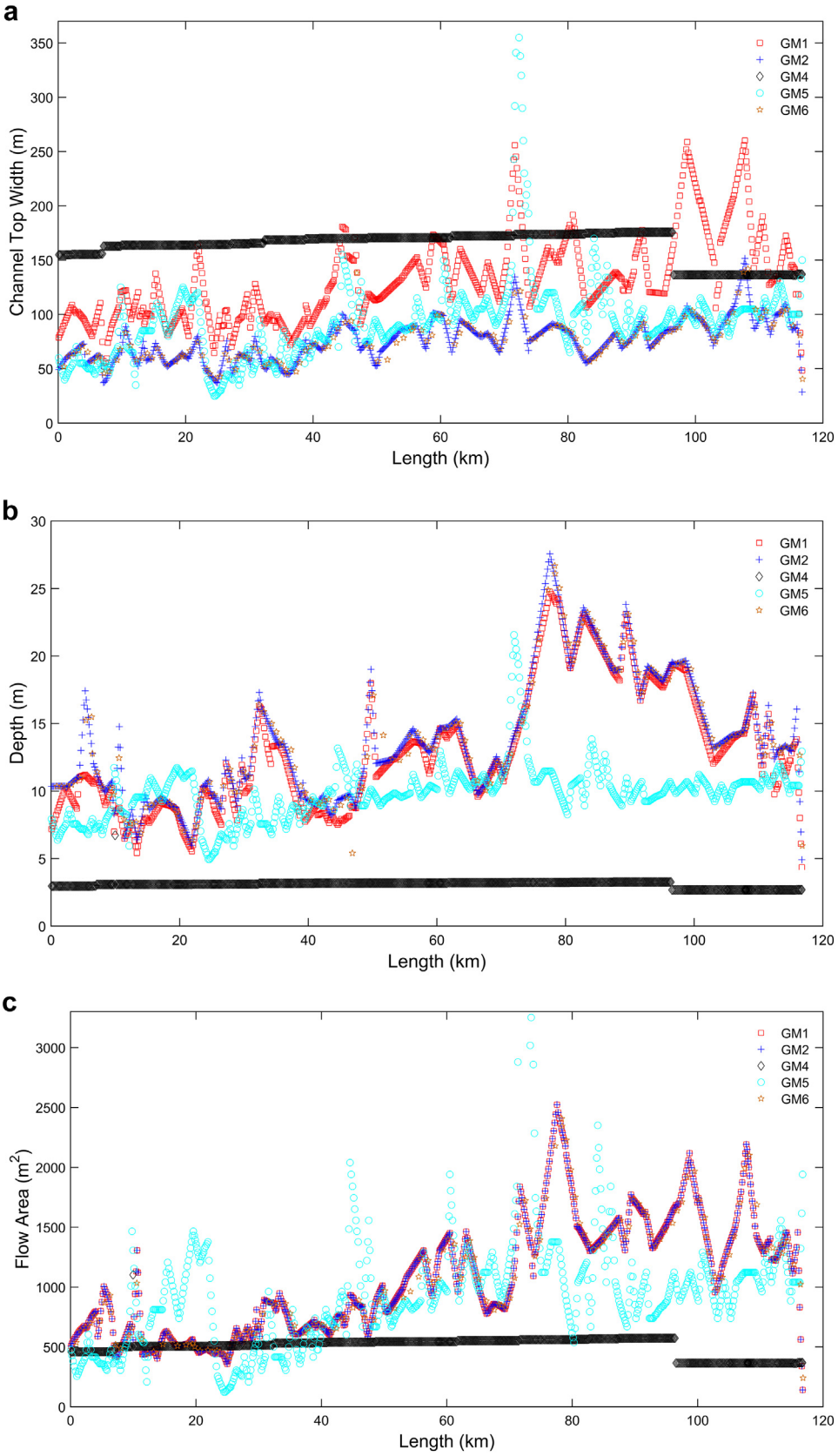

Fig. 5. Plots of channel (a) top width, (b) depth, and (c) flow area using different geomorphic models.

For better understanding the differences in flood depth simulation, the channel discharge profile (i.e. the flow going only through the 1D channel model) is investigated (Fig. 7). There is a clear dependence of the maximum channel discharge with the channel geometry model characterizing the 5 GMs (obviously the floodplain model GM3 is not considered). For example, GM2, and GM6 approximate the flow

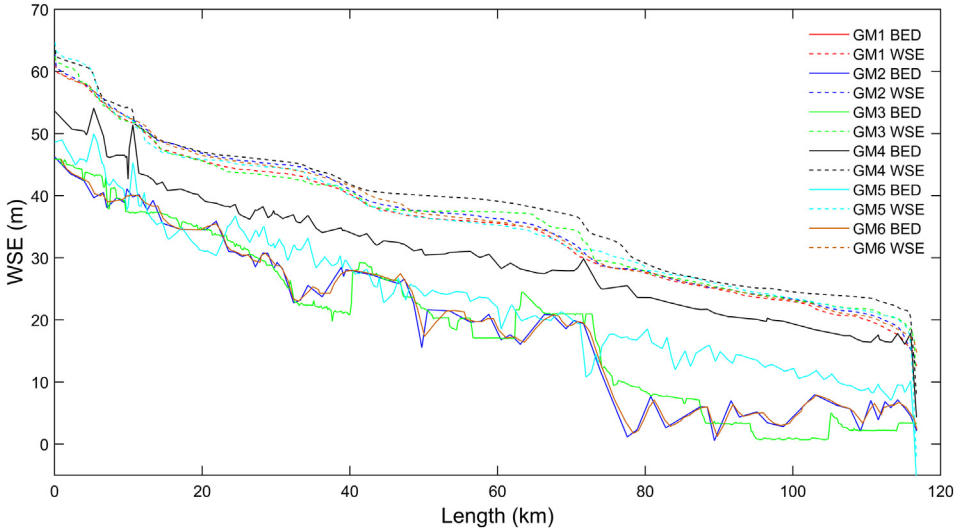

Fig. 6. River channel profile with simulated maximum water surface elevation (WSE) at a 150-m resolution and different geomorphic model approaches.

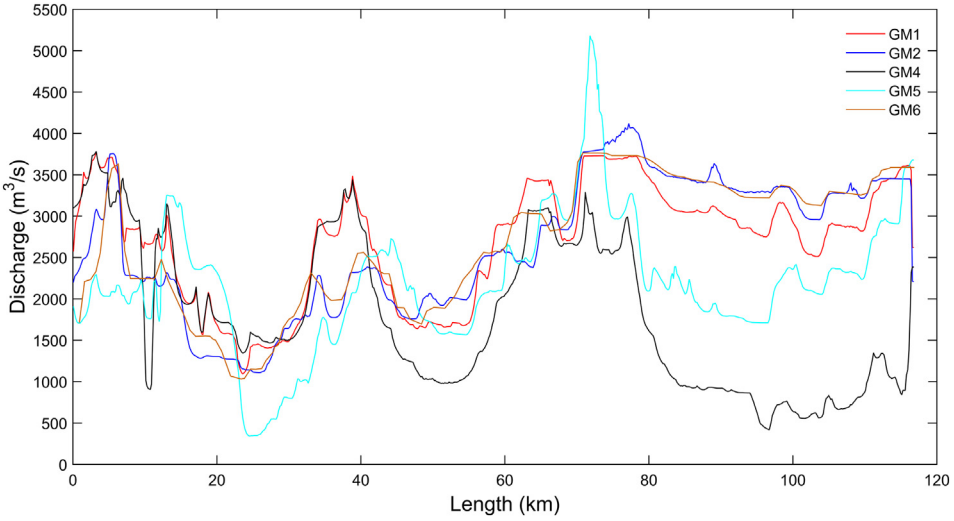

Fig. 7. River channel flow profile with simulated maximum peak discharge at a 150-m resolution and different model approaches.

propagation dynamics of the reference GM1 model. Although these methods preserve the flow area, depth and thalweg, modified channel cross section shapes and resolution can result in considerable differences along with the profile. Similarly, GM4, and GM5 behave according to their respective channel characteristics.

The visual comparison of the WSE in the river channel profile indicates that all approaches have consistent behavior, with the exception of GM4. The results suggest that it is possible to obtain reasonable flood depth and extent when simulating inundations corresponding to high return period flood events that significantly exceed the river channel capacity. This is expected considering the floodplain topography, rather than the channel bathymetry, acts as the governing factor of the inundation dynamics. Preserving the channel flow area is, in any case, the key parameter for more accurate and reliable simulations. It is worth noting that all GM approaches produce accurate approximations of inundation depths and extents (Fit index ≥ 0.90) compared to the reference model (Table 2). Although the hydrological GFHM has a higher resolution (100 m), the inundated area is slightly lower than the reference model. Conversely, the hydrogeomorphic GFHM based on the GFPLAIN250m dataset identifies the maximum extension of flood-prone areas by geomorphic scaling laws, overpredicting the inundated area. While GM1 to GM5 share the same 150 m resolution with similar degrees of running time from 15 to 30 min, coarser resolution models are more computationally efficient, resulting in the lower number of cells.

The description of the flood inundation mapping schemes using the 2D hydraulic model are presented in the following order: Fig. 8 presents the maximum flood inundation depth and extents of the reference model and GM approaches, highlighting the effect of bathymetry and model spatial resolution on the FLO-2D simulation. For example, GM2 is

Table 2
Performance metrics of running time, maximum simulated inundated area and F-index comparing reference model (GM1) with different geomorphic methods, and GFHM.

Grid size (m)	Number of cells	Running time (min)	RMSE (m)	Inundated area (m^2)	F-index (–)
GM1	11,191	23.01		120,555,000	
GM2	11,191	15.45	0.88	112,927,500	0.907
GM3	11,191	14.87	1.11	126,000,000	0.942
GM4	11,191	31.79	2.17	136,035,000	0.899
GM5	11,191	32.92	1.37	126,180,000	0.930
GM6	498	1.44	0.48	113,680,000	0.901
Hydrological				116,385,605	0.800
Hydrogeomorphic				163,375,620	

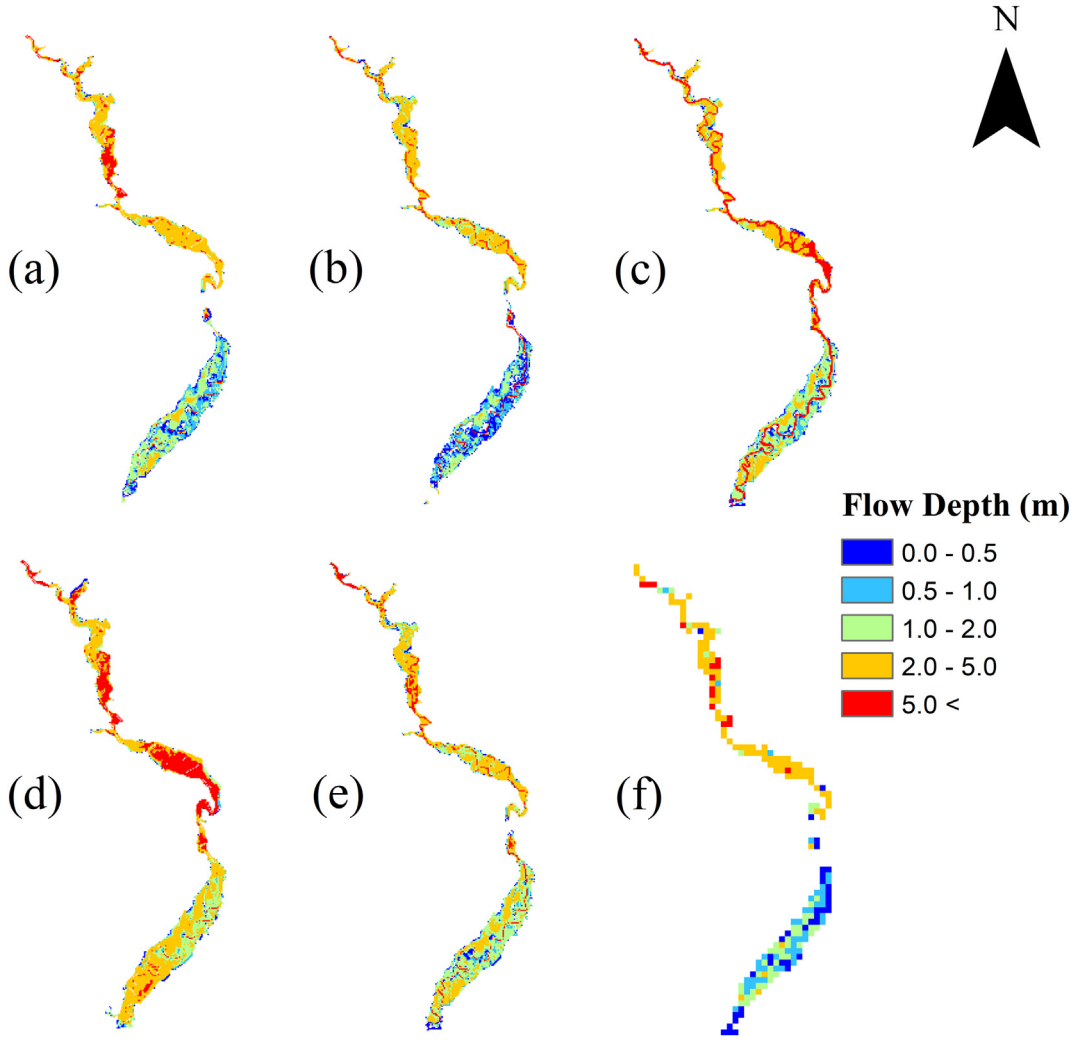

Fig. 8. Distribution of inundation flow depth for: (a) reference model at a 150-m resolution and natural cross sections GM1; as compared to geomorphic models: (b) GM2; (c) GM3; (d) GM4; (e) GM5; and (f) GM6.

slightly different to GM1 in terms of flood depth, due to the interpolation of natural cross sections to produce a rectangular channel bathymetric model. Similarly, GM3 and GM5 follow a consistent pattern, with minor differences during changes in slope. GM4 clearly overestimates the flood depth as a result of the limited flood area. Furthermore, the model resolution plays an essential role in the accurate depiction of the flood depth and extent of the entire domain (GM6). The postprocessing tool presented in Fig. 5 (step iv) is applied in Figs. 9–10 to produce 30 m high resolution inundation maps. Fig. 9 shows the spatial distribution of differences between the GM maximum WSE levels of the reference model (top), and the postprocessed higher resolution (bottom). Fig. 10 presents the maximum flood depth of the reference model (GM1) for the entire reach with three magnified samples located in the upstream, middle and downstream sections to compare the inundation depths in

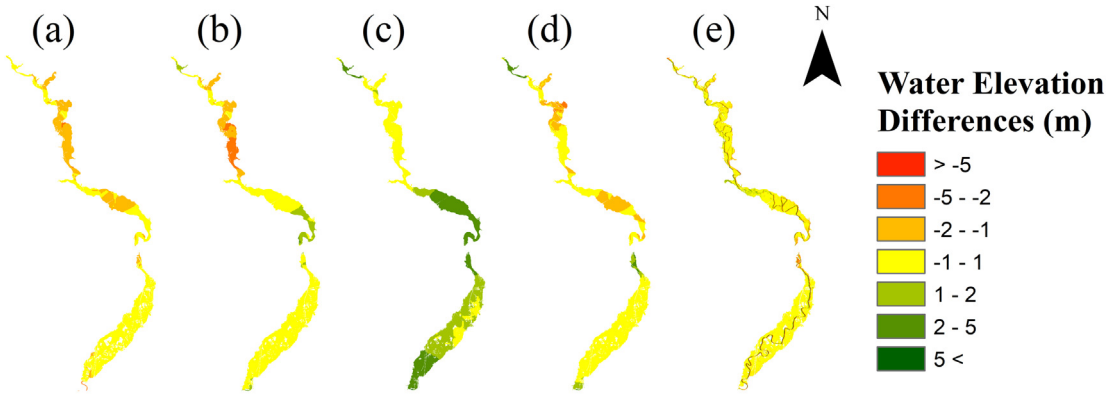

Fig. 9. Distribution of simulated surface water elevation differences for the defined model resolution models against the reference model using the 150-m model resolution (top) and the postprocessed 30 m resolution (bottom) with: (a) GM2; (b) GM3; (c) GM4; (d) GM5; and (e) GM6.

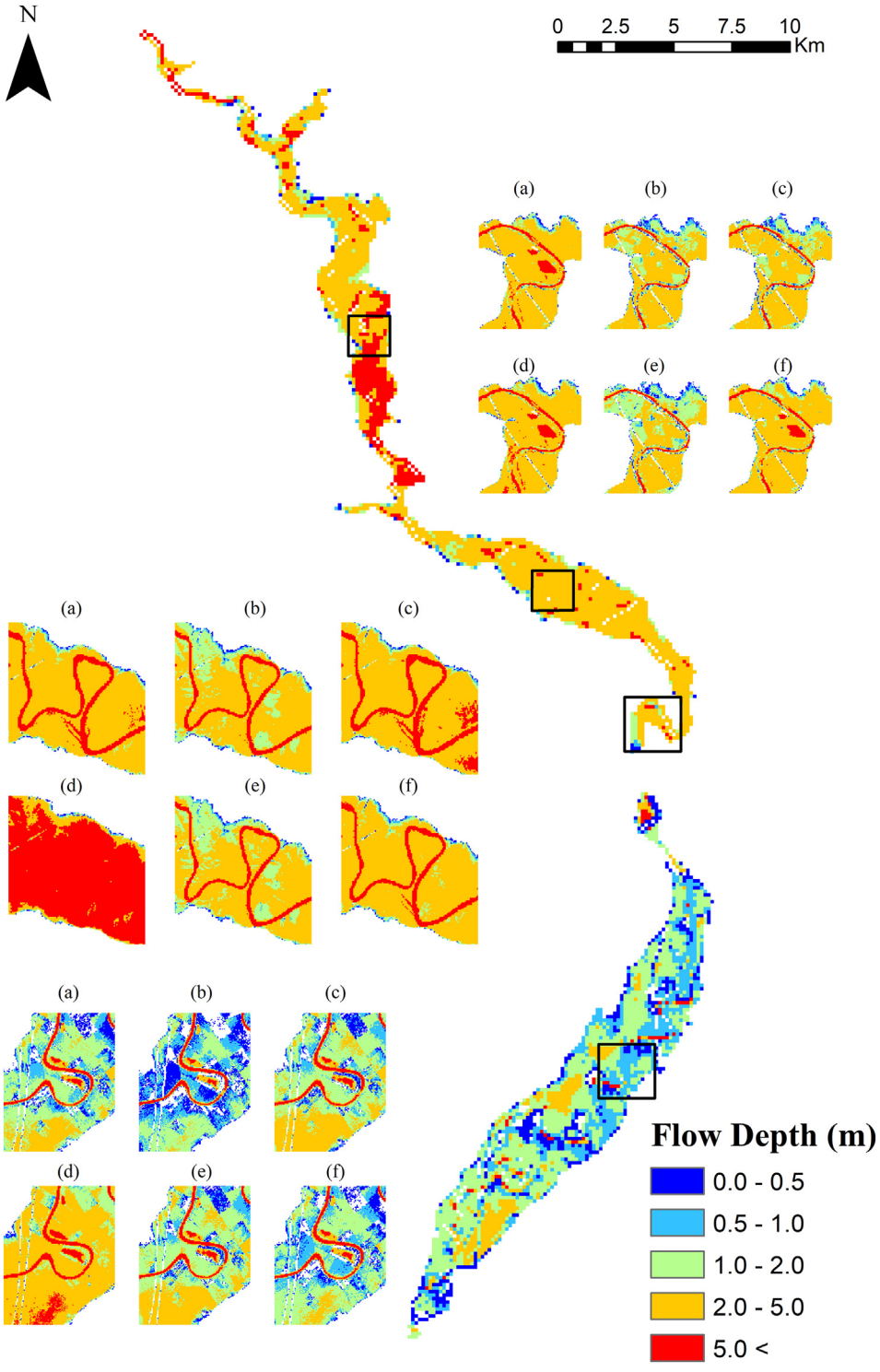

Fig. 10. Distribution of inundation flow depth of the reference model at a 150-m resolution (full-scale map) and three selected subdomains where inundation depths are depicted using the postprocessing geospatial algorithm for visualizing the different flood modelling scenario at 30 m model resolution comparing (a) reference model; (b) GM2; (c) GM3; (d) GM4; (e) GM5; and (f) GM6.

higher resolution. Fig. 11 displays the reference model's flood inundation extent at 150 m resolution, and both GFHMs.

Although the hydraulic flood map by Dottori et al. (2016) is consistent to GM1 in terms of flood extent, there are important overestimations in flow depth on the range of 2–5 m. A potential explanation could be attributed to the hydrological input from GloFAS simulations and the characterization of the hydrograph for a 200-years return period. On the other hand, the hydrogeomorphic flood map (GFPLAIN250m) by Nardi et al. (2019) captures the spatial extension of the floodplain by the identification of the fluvial valley zoning based on geomorphic scaling laws, producing a much higher inundated area for the area of study.

5. Discussion

The proposed research assessed the potential of selected geomorphic floodplain methods (GMs) and global flood hazard models

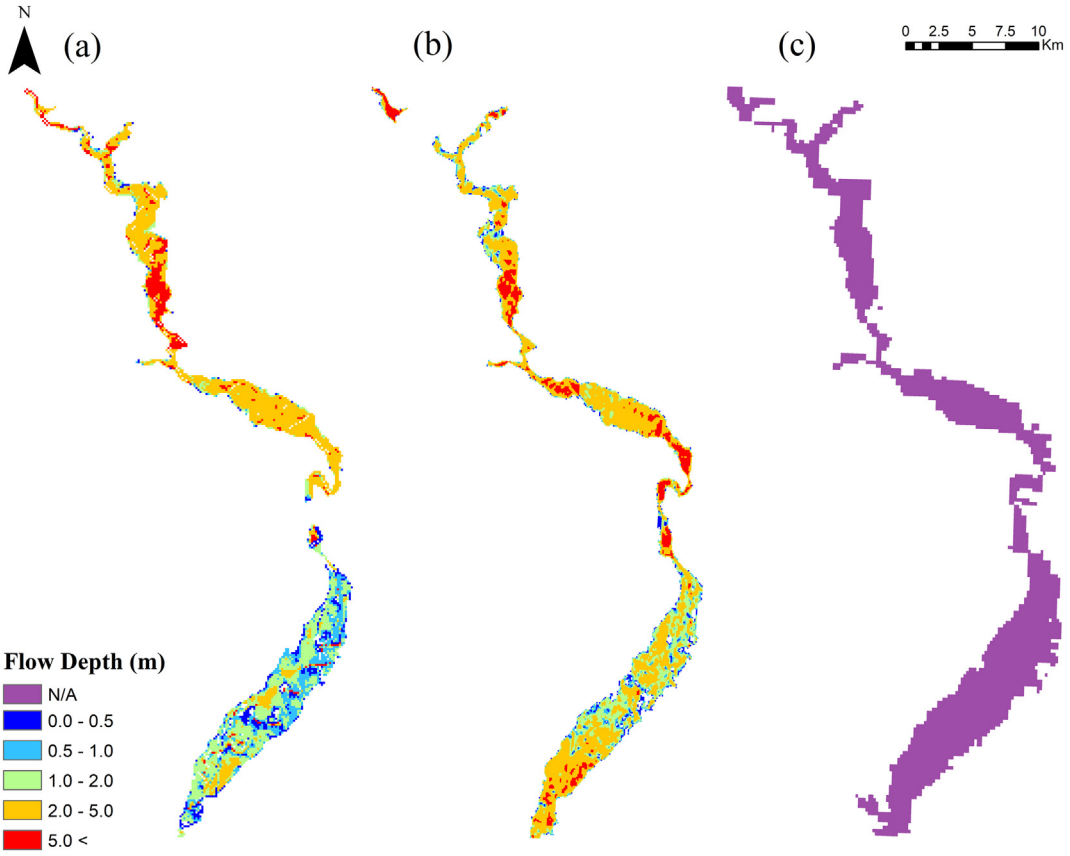

Fig. 11. Distribution of inundation flow depth comparing (a) reference model at a 150-m resolution; (b) hydraulic flood mapping (Dottori et al., 2016); and (c) hydromorphic flood mapping (Nardi et al., 2019). The hydrologic approach estimates water surface elevation with a return period of 200 years, while the hydrogeomorphic based on the GFPLAIN250m dataset only identifies the maximum extension of the flood-prone areas.

(GFHM) in a 2D hydrodynamic model, with specific regard on using coarser resolutions under extreme flood conditions to produce fast and consistent large-scale flood simulations.

The estimation of river bathymetry is of relevant significance to the hydraulic modelling community, in particular for the production of flood inundation maps which often deal with challenges connected to limited or lack of channel geometry data. Several studies have investigated the use of remote sensing techniques (Biancamaria et al., 2016; Moramarco et al., 2019), hydraulic geometry relations (Andreadis et al., 2020; Choné et al., 2018) and geomorphic laws (Leopold and Maddock, 1953) in the production of synthetic cross sections through simple geometric shapes (i.e. rectangular, trapezoidal, parabolic) as a proxy to preserve the channel-conveyance capacity and thalweg profile at different scales (Glenn et al., 2016; Neal et al., 2015; Trigg et al., 2009).

The development of coarser resolution models has received significantly less attention compared to high-resolution models due to the technological and scientific breakthroughs in Earth Observation (EO) and Geo-Information Science, which are constantly improving the quality of DTMs used for the development of detailed flood mapping products. Although finer mesh resolutions are preferred over coarser resolution to achieve more precision and accuracy, an adequate balance between the model's complexity and detail is critical to seize the model output predictions and performance metrics for specific applications (Alfieri et al., 2014; Bates et al., 2003; Casas et al., 2006; Hunter et al., 2007; Neal et al., 2010; Prodanović et al., 2009; Schumann et al., 2018; Wing et al., 2017; Yu and Lane, 2011).

This research posits the question of how much DEM uncertainties affect the inundation extents and depths in large scale applications. Results show that all geomorphic models produced fairly accurate flood inundation depths and extents (Fit index ≥ 0.90), while the overestimation of flow depths are attributed to the differences in the channel geometry and bed profile (e.g., Fig. 7). As for the GFHM, both global flood maps are consistent to the flood inundation levels and extend to the benchmark reference model (Fig. 11), proving cost-effective for regions with limited resources and technical expertise.

In this context, the proposed procedure by Peña and Nardi (2018) represents a computationally efficient approach to simulate the return period of extreme hydrologic events over large floodplains. The ability to simulate multiple flood scenarios in minutes represents a considerable advantage in flood preparedness and response operations as first responders can identify in advance the timing of flood levels and spatial distribution allowing for effective evacuation procedures and warnings (Gilissen et al., 2016; Longenecker et al., 2020; Teng et al., 2015). Similarly, the postprocessing of simulated water surface elevations model may prove beneficial to support detailed socio-economic and environmental management studies (Fluet-Chouinard et al., 2015).

Nevertheless, the proposed floodplain terrain resampling framework and geomorphic methods present evident limitations related to the terrain accuracy and inundation areas compared to high-resolution flood models, as well as manual processing work that can be cumbersome and subject to human-induced errors. Further research on the use of machine learning algorithms for model development and optimization could result in a substantial increase of automated approaches for flood prediction in the future (Mosavi et al., 2018). Future work on assessing the impact of topographic and bathymetric uncertainties in coarser resolution models could be addressed on quantitative comparisons of floodplain and channel conveyance by simulating high and low probability events using 1D and 2D modelling approaches (Cook and Merwade, 2009; Saksena et al., 2020).

6. Conclusions

This research investigated the characterization of fluvial bathymetry by means of geomorphic methods and its applications for real time emergency management operations using the 2D hydrodynamic model FLO-2D. The application of geomorphic methods was tested on the 120 km domain of the Tiber middle valley to evaluate their ability (or inefficiency) of surrogating the lack of surveyed fluvial bathymetric data as compared to a validated reference model with channel cross sections. The presented methods do not aim to replicate the performance of surveyed fluvial bathymetry in large-scale coarser domains, but to remain as an alternative approach for the development of parsimonious flood models in data-scarce regions. Similarly, the hydraulic and hydrogeomorphic global products can be seen as a complementary tool for flood risk delineation. Overall, the performance metrics showed that differences in fluvial geomorphic configurations lead to uncertainties in the channel-floodplain interactions and flow dynamics, highlighting the effects of the DEM in the vertical accuracy of coarser-resolution models. Conversely, small-scale features and river bathymetry are negligible under extreme hydrologic events as the floodplain conveyance capacity is the driving principle of flood inundation dynamics. Under these conditions, geomorphic floodplain coarse resolutions models are suitable to produce fast and consistent distributions of inundation depths and extent in large domains. The replicability of this study in other river basins using different return periods and coarser resolutions may provide valuable insights on the effectiveness and limitations of geomorphic laws and global flood hazard maps in respect to high-resolution models.

Funding

This work was supported by the University for Foreigners of Perugia — ISPRA-INFO/RAC2020 Research Grant No. COAN AC.11.04.01 (Research grant "Research and implementation of GIS and hydrologic-hydraulic models for large scale water and flood risk management to support the Disaster Risk Reduction program"). In addition, this material is based upon work supported by the National Science Foundation under Grant No. HRD-1547798. This NSF Grant was awarded to Florida International University as part of the Centers for Research Excellence in Science and Technology (CREST) Program. This is contribution number 1024 from the Southeast Environmental Research Center in the Institute of Environment at Florida International University. This work was also funded by Florida International University Sea Level Solution Center Grant No. 800008174, and the Dissertation Year Fellowship from the FIU University Graduate School.

Declaration of competing interest

The authors declare that they have no known competing financial interests or personal relationships that could have appeared to influence the work reported in this paper.

References

Alfieri, L., Salamon, P., Bianchi, A., Neal, J., Bates, P., Feyen, L., 2014. Advances in pan-European flood hazard mapping. Hydrol. Process. 28, 4067–4077. https://doi.org/10.1002/hyp.9947.

Alfieri, L., Bisselink, B., Dottori, F., Naumann, G., Roo, A., Salamon, P., Wyser, K., Feyen, L., 2017. Global projections of river flood risk in a warmer world. Earth's Fut. 5, 171–182. https://doi.org/10.1002/2016EF000485.

Altenau, E.H., Pavelsky, T.M., Bates, P.D., Neal, J.C., 2017. The effects of spatial resolution and dimensionality on modeling regional-scale hydraulics in a multichannel river. Water Resour. Res. 53, 1683–1701. https://doi.org/10.1002/2016WR019396.

Andreadis, K.M., Schumann, G.J.P., Pavelsky, T., 2013. A simple global river bankfull width and depth database. Water Resour. Res. 49, 7164–7168. https://doi.org/10.1002/wrcr.20440.

Andreadis, K.M., Brinkerhoff, C.B., Gleason, C.J., 2020. Constraining the assimilation of SWOT observations with hydraulic geometry relations. Water Resour. Res. 56, 1–21. https://doi.org/10.1029/2019WR026611.

Annis, A., Nardi, F., 2019. Integrating VGI and 2D hydraulic models into a data assimilation framework for real time flood forecasting and mapping. Geo-Spat. Inf. Sci. 22, 223–236. https://doi.org/10.1080/10095020.2019.1626135.

Annis, A., Nardi, F., Morrison, R.R., Castelli, F., 2019. Investigating hydrogeomorphic floodplain mapping performance with varying DTM resolution and stream order. Hydrol. Sci. J. 64, 525–538. https://doi.org/10.1080/02626667.2019.1591623.

Annis, A., Nardi, F., Petroselli, A., Apollonio, C., Arcangeletti, E., Tauro, F., Belli, C., Bianconi, R., Grimaldi, S., 2020a. UAV-DEMs for small-scale flood hazard mapping. Water (Switzerland) 12. https://doi.org/10.3390/w12061717.

Annis, A., Nardi, F., Volpi, E., Fiori, A., 2020b. Quantifying the relative impact of hydrological and hydraulic modelling parameterizations on uncertainty of inundation maps. Hydrol. Sci. J. 65, 507–523. https://doi.org/10.1080/02626667.2019.1709640.

Aronica, G., Bates, P.D., Horritt, M.S., 2002. Assessing the uncertainty in distributed model predictions using observed binary pattern information within GLUE. Hydrol. Process. 16, 2001–2016. https://doi.org/10.1002/hyp.398.

Barnard, P.L., Erikson, L.H., Kvitek, R.G., 2011. Small-scale sediment transport patterns and bedform morphodynamics: new insights from high-resolution multibeam bathymetry. Geo-Mar. Lett. 31, 227–236. https://doi.org/10.1007/s00367-011-0227-1.

Bates, P.D., 2012. Integrating remote sensing data with flood inundation models: how far have we got? Hydrol. Process 26, 2515–2521. https://doi.org/10.1002/hyp.9374.

Bates, P.D., De Roo, A.P.J., 2000. A simple raster-based model for flood inundation simulation. J. Hydrol. 236, 54–77. https://doi.org/10.1016/S0022-1694(00)00278-X.

Bates, P.D., Marks, K.J., Horritt, M.S., 2003. Optimal use of high-resolution topographic data in flood inundation models. Hydrol. Process. 17, 537–557. https://doi.org/10.1002/hyp.1113.

Bates, P.D., Dawson, R.J., Hall, J.W., Horritt, M.S., Nicholls, R.J., Wicks, J., Ali Mohamed Hassan, M.A., 2005. Simplified two-dimensional numerical modelling of coastal flooding and example applications. Coast. Eng. 52, 793–810. https://doi.org/10.1016/j.coastaleng.2005.06.001.

Bhola, P.K., Leandro, J., Disse, M., 2018. Framework for offline flood inundation forecasts for two-dimensional hydrodynamic models. Geosci. 8. https://doi.org/10.3390/geosciences8090346.

Bhowmik, N.G., Stall, J.B., 1979. Hydraulic Geometry and Carrying Capacity of Floodplains.

Bhuyian, M.N.M., Kalyanapu, A.J., Nardi, F., 2015. Approach to digital elevation model correction by improving channel conveyance. J. Hydrol. Eng. 20, 1–10. https://doi.org/10.1061/(ASCE)HE.1943-5584.0001020.

Biancamaria, S., Bates, P.D., Boone, A., Mognard, N.M., 2009. Large-scale coupled hydrologic and hydraulic modelling of the Ob river in Siberia. J. Hydrol. 379, 136–150. https://doi.org/10.1016/j.jhydrol.2009.09.054.

Biancamaria, S., Lettenmaier, D.P., Pavelsky, T.M., 2016. The SWOT mission and its capabilities for land hydrology. Surv. Geophys. 37, 307–337. https://doi.org/10.1007/s10712-015-9346-y.

Bierkens, M.F.P., 2015. Global hydrology 2015: state, trends, and directions. Water Resour. Res., 4923–4947 https://doi.org/10.1002/2015WR017173.

Brandt, S.A., 2005. Resolution issues of elevation data during inundation modeling of river floods. XXXI Int. Assoc. Hydraul. Eng. Res. Congr, pp. 3573–3581.

Burby, R.J., 2006. Hurricane Katrina and the paradoxes of government disaster policy: bringing about wise governmental decisions for hazardous areas. Ann. Am. Acad. Pol. Soc. Sci. 604, 171–191. https://doi.org/10.1177/0002716205284676.

Casas, A., Benito, G., Thorndycraft, V.R., Rico, M., 2006. The topographic data source of digital terrain models as a key element in the accuracy of hydraulic flood modelling. Earth Surf. Process. Landf. 31, 444–456. https://doi.org/10.1002/esp.1278.

Chau, V.N., Holland, J., Cassells, S., Tuohy, M., 2013. Using GIS to map impacts upon agriculture from extreme floods in Vietnam. Appl. Geogr. 41, 65–74. https://doi.org/10.1016/j.apgeog.2013.03.014.

Choné, G., Biron, P.M., Buffin-Bélanger, T., 2018. Flood hazard mapping techniques with LiDAR in the absence of river bathymetry data. E3S Web Conf. 40.

Cobby, D.M., Mason, D.C., Davenport, I., 2001. Image processing of airborne scanning laser altimetry data for improved river flood modelling. ISPRS J. Photogramm. Remote Sens. 56, 121–138. https://doi.org/10.1016/S0924-2716(01)00039-9.

Convertino, M., Annis, A., Nardi, F., 2019. Information-theoretic portfolio decision model for optimal flood management. Environ. Model. Softw. 119, 258–274. https://doi.org/10.1016/j.envsoft.2019.06.013.

Cook, A., Merwade, V., 2009. Effect of topographic data, geometric configuration and modeling approach on flood inundation mapping. J. Hydrol. 377, 131–142. https://doi.org/10.1016/j.jhydrol.2009.08.015.

Dey, S., Saksena, S., Merwade, V., 2019. Assessing the effect of different bathymetric models on hydraulic simulation of rivers in data sparse regions. J. Hydrol. 575, 838–851. https://doi.org/10.1016/j.jhydrol.2019.05.085.

Di Baldassarre, G., Schumann, G., Brandimarte, L., Bates, P., 2011. Timely low resolution SAR imagery to support floodplain modelling: a case study review. Surv. Geophys. 32, 255–269. https://doi.org/10.1007/s10712-011-9111-9.

Di Baldassarre, G., Nohrstedt, D., Mård, J., Burchardt, S., Albin, C., Bondesson, S., Breinl, K., Deegan, F.M., Fuentes, D., Lopez, M.G., Granberg, M., Nyberg, L., Nyman, M.R., Rhodes, E., Troll, V., Young, S., Walch, C., Parker, C.F., 2018. An integrative research framework to unravel the interplay of natural hazards and vulnerabilities. Earth's Fut. 6, 305–310. https://doi.org/10.1002/2017EF000764.

Di Baldassarre, G., Nardi, F., Annis, A., Odongo, V., Rusca, M., Grimaldi, S., 2020. Brief communication: comparing hydrological and hydrogeomorphic paradigms for global flood hazard mapping. Nat. Hazards Earth Syst. Sci. 20, 1415–1419. https://doi.org/10.5194/nhess-20-1415-2020.

Di, L., Yu, E.G., Kang, L., Shrestha, R., BAI, Y., 2017. RF-CLASS: a remote-sensing-based flood crop loss assessment cyber-service system for supporting crop statistics and insurance decision-making. J. Integr. Agric. 16, 408–423. https://doi.org/10.1016/S2095-3119(16)61499-5.

Dingman, S.L., 2009. Fluvial Hydraulics. 1st ed. Oxford University Press.

Dodov, B., Foufoula-Georgiou, E., 2004. Generalized hydraulic geometry: derivation based on a multiscaling formalism. Water Resour. Res. 40, 1–22. https://doi.org/10.1029/2003WR002082.
Domeneghetti, A., 2016. On the use of SRTM and altimetry data for flood modeling in data-sparse regions. Water Resour. Res. 52, 2901–2918. https://doi.org/10.1002/2015WR017967.
Doocy, S., Daniels, A., Murray, S., Kirsch, T., 2013. The Human Impact of Floods: A Historical Review of Events 1980–2009 and Systematic Literature Review. https://doi.org/10.1371/currents.dis.f4deb457904936b07c09daa98ee8171a.
Dottori, F., Di Baldassarre, G., Todini, E., 2013. Detailed data is welcome, but with a pinch of salt: accuracy, precision, and uncertainty in flood inundation modeling. Water Resour. Res. 49, 6079–6085. https://doi.org/10.1002/wrcr.20406.
Dottori, F., Salamon, P., Bianchi, A., Alfieri, L., Hirpa, F.A., Feyen, L., 2016. Development and evaluation of a framework for global flood hazard mapping. Adv. Water Resour 94, 87–102. https://doi.org/10.1016/j.advwatres.2016.05.002.
Dottori, F., Kalas, M., Salamon, P., Bianchi, A., Alfieri, L., Feyen, L., 2017. An operational procedure for rapid flood risk assessment in Europe. Nat. Hazards Earth Syst. Sci. 17, 1111–1126. https://doi.org/10.5194/nhess-17-1111-2017.
Dottori, F., Szewczyk, W., Ciscar, J.C., Zhao, F., Alfieri, L., Hirabayashi, Y., Bianchi, A., Mongelli, I., Frieler, K., Betts, R.A., Feyen, L., 2018. Increased human and economic losses from river flooding with anthropogenic warming. Nat. Clim. Chang. 8, 781–786. https://doi.org/10.1038/s41558-018-0257-z.
ESRI, 2011. ArcGIS Desktop: Release 10.
Farr, T.G., Rosen, P.A., Caro, E., Crippen, R., Duren, R., Hensley, S., Kobrick, M., Paller, M., Rodriguez, E., Roth, L., Seal, D., Shaffer, S., Shimada, J., Umland, J., Werner, M., Oskin, M., Burbank, D., Alsdorf, D.E., 2007. The shuttle radar topography mission. Rev. Geophys. 45. https://doi.org/10.1029/2005RG000183.
Fluet-Chouinard, E., Lehner, B., Rebelo, L.-M., Papa, F., Hamilton, S.K., 2015. Development of a global inundation map at high spatial resolution from topographic downscaling of coarse-scale remote sensing data. Remote Sens. Environ. 158, 348–361. https://doi.org/10.1016/j.rse.2014.10.015.
Gan, T.Y., Zunic, F., Kuo, C.C., Strobl, T., 2012. Flood mapping of Danube river at Romania using single and multi-date ERS2-SAR images. Int. J. Appl. Earth Obs. Geoinf. 18, 69–81. https://doi.org/10.1016/j.jag.2012.01.012.
Gichamo, T.Z., Popescu, I., Jonoski, A., Solomatine, D., 2012. River cross-section extraction from the ASTER global DEM for flood modeling. Environ. Model. Softw. 31, 37–46. https://doi.org/10.1016/j.envsoft.2011.12.003.
Gilissen, H.K., Alexander, M., Matczak, P., Pettersson, M., Bruzzone, S., 2016. A framework for evaluating the effectiveness of flood emergency management systems in Europe. Ecol. Soc. 21.
Glenn, J., Tonina, D., Morehead, M.D., Fiedler, F., Benjankar, R., 2016. Effect of transect location, transect spacing and interpolation methods on river bathymetry accuracy. Earth Surf. Process. Landf. 41, 1185–1198. https://doi.org/10.1002/esp.3891.
Grimaldi, S., Teles, V., Bras, R.L., 2004. Sensitivity of a physically based method for terrain interpolation to initial conditions and its conditioning on stream location. Earth Surf. Process. Landf. 29, 587–597. https://doi.org/10.1002/esp.1053.
Grimaldi, S., Teles, V., Bras, R.L., 2005. Preserving first and second moments of the slope area relationship during the interpolation of digital elevation models. Adv. Water Resour. 28, 583–588. https://doi.org/10.1016/j.advwatres.2004.11.014.
Grimaldi, S., Li, Y., Walker, J.P., Pauwels, V.R.N., 2018. Effective representation of river geometry in hydraulic flood forecast models. Water Resour. Res. 54, 1031–1057. https://doi.org/10.1002/2017WR021765.
Henonin, J., Russo, B., Mark, O., Gourbesville, P., 2013. Real-time urban flood forecasting and modelling — a state of the art. J. Hydroinf. 15, 717–736. https://doi.org/10.2166/hydro.2013.132.
Hey, R.D., Thorne, C.R., 1986. Stable channels with mobile gravel beds. J. Hydraul. Eng. 112, 671–689. https://doi.org/10.1061/(ASCE)0733-9429(1988)114:3(339).
Hilldale, R.C., Raff, D., 2008. Assessing the ability of airborne LiDAR to map river bathymetry. Earth Surf. Process. Landf. 33, 773–783. https://doi.org/10.1002/esp1575.
Hunter, N.M., Bates, P.D., Horritt, M.S., Wilson, M.D., 2007. Simple spatially-distributed models for predicting flood inundation: a review. Geomorphology 90, 208–225. https://doi.org/10.1016/j.geomorph.2006.10.021.
Ignacio, J.A.F., Cruz, G.T., Nardi, F., Henry, S., 2015. Assessing the effectiveness of a social vulnerability index in predicting heterogeneity in the impacts of natural hazards: case study of the Tropical Storm Washi flood in the Philippines. Vienna Yearb. Popul. Res. 1, 91–129. https://doi.org/10.1553/populationyearbook2015s91.
IPCC, 2014. Climate change 2014. Synthesis Report. Contribution of Working Groups I, II and III to the Fifth Assessmetn Report of the Intergovernmental Panel on Climate Change Geneva, Switzerland.
Jonkman, S.N., Bočkarjova, M., Kok, M., Bernardini, P., 2008. Integrated hydrodynamic and economic modelling of flood damage in the Netherlands. Ecol. Econ. 66, 77–90. https://doi.org/10.1016/j.ecolecon.2007.12.022.
Jung, H.C., Hamski, J., Durand, M., Alsdorf, D., Hossain, F., Lee, H., Azad Hossain, A.K.M., Hasan, K., Khan, A.S., Zeaul Hoque, A.K.M., 2010. Characterization of complex fluvial systems using remote sensing of spatial and temporal water level variations in the Amazon, Congo, and Brahmaputra rivers. Earth Surf. Process. Landf. 35, 294–304. https://doi.org/10.1002/esp.1914.
Kam, P.M., Aznar-Siguan, G., Schewe, J., Milano, L., Ginnetti, J., Willner, S., McCaughey, J.W., Bresch, D.N., 2021. Global warming and population change both heighten future risk of human displacement due to river floods. Environ. Res. Lett. 16, 44026. https://doi.org/10.1088/1748-9326/abd26c.
Kasvi, E., Salmela, J., Lotsari, E., Kumpula, T., Lane, S.N., 2019. Comparison of remote sensing based approaches for mapping bathymetry of shallow, clear water rivers. Geomorphology 333, 180–197. https://doi.org/10.1016/j.geomorph.2019.02.017.
Knighton, A.D., 1975. Variations in at-a-station hydraulic geometry. Am. J. Sci. https://doi.org/10.2475/ajs.275.2.186.
Lehner, B., Verdin, K., Jarvis, A., 2008. New global hydrography derived from spaceborne elevation data. Eos (Washington, DC). 89, 93–94. https://doi.org/10.1029/2008EO100001.
Leopold, L., Maddock, T., 1953. The Hydraulic Geometry of Stream Channels and Some Physiographic Implications.
Leskens, J.G., Brugnach, M., Hoekstra, A.Y., Schuurmans, W., 2014. Why are decisions in flood disaster management so poorly supported by information from flood models? Environ. Model. Softw. 53, 53–61. https://doi.org/10.1016/j.envsoft.2013.11.003.
Lewis, L.A., 1969. Some fluvial geomorphic characteristics of the Manati Basin, Puerto Rico. Ann. Assoc. Am. Geogr. 59, 280–293. https://doi.org/10.1111/j.1467-8306.1969.tb00671.x.
Longenecker, H.E., Graeden, E., Kluskiewicz, D., Zuzak, C., Rozelle, J., Aziz, A.L., 2020. A rapid flood risk assessment method for response operations and nonsubject-matter-expert community planning. J. Flood Risk Manag. 13, 1–20. https://doi.org/10.1111/jfr3.12579.
Löwe, R., Urich, C., Sto. Domingo, N., Mark, O., Deletic, A., Arnbjerg-Nielsen, K., 2017. Assessment of urban pluvial flood risk and efficiency of adaptation options through simulations — a new generation of urban planning tools. J. Hydrol. 550, 355–367. https://doi.org/10.1016/j.jhydrol.2017.05.009.
Maidment, D.R., Djokic, D., 2000. Hydrologic and Hydraulic Modeling Support: With Geographic Information Systems.
Manfreda, S., Nardi, F., Samela, C., Grimaldi, S., Taramasso, A.C., Roth, G., Sole, A., 2014. Investigation on the use of geomorphic approaches for the delineation of flood prone areas. J. Hydrol. 517, 863–876. https://doi.org/10.1016/j.jhydrol.2014.06.009.
Manfreda, S., McCabe, M., Miller, P., Lucas, R., Pajuelo Madrigal, V., Mallinis, G., Ben Dor, E., Helman, D., Estes, L., Ciraolo, G., Müllerová, J., Tauro, F., de Lima, M., de Lima, J., Maltese, A., Frances, F., Caylor, K., Kohv, M., Perks, M., Ruiz-Pérez, G., Su, Z., Vico, G., Toth, B., 2018. On the use of unmanned aerial systems for environmental monitoring. Remote Sens. 10, 641. https://doi.org/10.3390/rs10040641.
Marco, J.B., 1994. Flood risk mapping. Cop. With Flood. https://doi.org/10.1007/978-94-011-1098-3_20.
Mejia, A.I., Reed, S.M., 2011. Role of channel and floodplain cross-section geometry in the basin response. Water Resour. Res. 47, 1–15. https://doi.org/10.1029/2010WR010375.
Miller, J.P., 1958. High-Mountain Streams: Effects of Geology on Channel Characteristics and Bed Material (No. 4).
Montanari, A., 2012. Hydrology of the Po River: looking for changing patterns in river discharge. Hydrol. Earth Syst. Sci. 16, 3739–3747. https://doi.org/10.5194/hess-16-3739-2012.
Moody, J.A., Troutman, B.M., 2002. Characterization of the spatial variability of channel morphology. Earth Surf. Process. Landf. 27, 1251–1266. https://doi.org/10.1002/esp.403.
Moramarco, T., Barbetta, S., Bjerklie, D.M., Fulton, J.W., Tarpanelli, A., 2019. River bathymetry estimate and discharge assessment from remote sensing. Water Resour. Res. 55, 6692–6711. https://doi.org/10.1029/2018WR024220.
Mosavi, A., Ozturk, P., Chau, K., 2018. Flood prediction using machine learning models: literature review. Water https://doi.org/10.3390/w10111536.
Nardi, F., Vivoni, E.R., Grimaldi, S., 2006. Investigating a floodplain scaling relation using a hydrogeomorphic delineation method. Water Resour. Res. 42. https://doi.org/10.1029/2005WR004155.
Nardi, F., Annis, A., Biscarini, C., 2018a. On the impact of urbanization on flood hydrology of small ungauged basins: the case study of the Tiber river tributary network within the city of Rome. J. Flood Risk Manag. 11, S594–S603. https://doi.org/10.1111/jfr3.12186.
Nardi, F., Morrison, R.R., Annis, A., Grantham, T.E., 2018b. Hydrologic scaling for hydrogeomorphic floodplain mapping: Insights into human-induced floodplain disconnectivity. River Res. Appl., 1–11 https://doi.org/10.1002/rra.3296.
Nardi, F., Annis, A., Di Baldassarre, G., Vivoni, E.R., Grimaldi, S., 2019. GFPLAIN250m, a global high-resolution dataset of earth's floodplains. Sci. Data 6, 1–6. https://doi.org/10.1038/sdata.2018.309.
Neal, J., Schumann, G., Bates, P., 2012. A subgrid channel model for simulating river hydraulics and floodplain inundation over large and data sparse areas. Water Resour. Res. 48, 1–16. https://doi.org/10.1029/2012WR012514.
Neal, J.C., Fewtrell, T.J., Bates, P.D., Wright, N.G., 2010. A comparison of three parallelisation methods for 2D flood inundation models. Environ. Model. Softw. 25, 398–411. https://doi.org/10.1016/j.envsoft.2009.11.007.
Neal, J.C., Odoni, N.A., Trigg, M.A., Freer, J.E., Garcia-Pintado, J., Mason, D.C., Wood, M., Bates, P.D., 2015. Efficient incorporation of channel cross-section geometry uncertainty into regional and global scale flood inundation models. J. Hydrol. 529, 169–183. https://doi.org/10.1016/j.jhydrol.2015.07.026.
O'Brien, J.S., 2011. FLO-2D Users Manual.
O'Brien, J.S., Julien, P.Y., Fullerton, W.T., ASCE, M., 1993. Two-dimensional water flood and mudflow simulation. J. Hydraul. Eng. 119, 244–261.
Papaioannou, G., Loukas, A., Vasiliades, L., Aronica, G.T., 2016. Flood inundation mapping sensitivity to riverine spatial resolution and modelling approach. Nat. Hazards 83, 117–132. https://doi.org/10.1007/s11069-016-2382-1.
Pappenberger, F., Dutra, E., Wetterhall, F., Cloke, H.L., 2012. Deriving global flood hazard maps of fluvial floods through a physical model cascade. Hydrol. Earth Syst. Sci. 16, 4143–4156. https://doi.org/10.5194/hess-16-4143-2012.
da Paz, A.R., Collischonn, W., Tucci, C.E.M., Padovani, C.R., 2011. Large-scale modelling of channel flow and floodplain inundation dynamics and its application to the Pantanal (Brazil). Hydrol. Process. 25, 1498–1516. https://doi.org/10.1002/hyp.7926.
Peña, F., Nardi, F., 2018. Floodplain terrain analysis for coarse resolution 2D flood modeling. Hydrology 5. https://doi.org/10.3390/hydrology5040052.
Pistrika, A., 2010. Flood damage estimation based on flood simulation scenarios and a GIS platform. Eur. Water 30, 3–11.

Prodanović, D., Stanić, M., Milivojević, V., Simić, Z., Arsić, M., 2009. DEM-based GIS algorithms for automatic creation of hydrological models data. J. Serb. Soc. Comput. Mech. 3, 64–85.
Reichenbach, P., Cardinali, M., De Vita, P., Guzzetti, F., 1998. Regional hydrological thresholds for landslides and floods in the Tiber River Basin (central Italy). Environ. Geol. 35, 146–159. https://doi.org/10.1007/s002540050301.
Saksena, S., Merwade, V., 2015. Incorporating the effect of DEM resolution and accuracy for improved flood inundation mapping. J. Hydrol. 530, 180–194. https://doi.org/10.1016/j.jhydrol.2015.09.069.
Saksena, S., Merwade, V., 2017. Integrated modeling of surface-subsurface processes to understand river-floodplain hydrodynamics in the Upper Wabash river basin. Perspect. Hist. Heritage, Emerg. Technol. Student Pap. - Sel. Pap. From World Environ. Water Resour. Congr, pp. 60–68 https://doi.org/10.1061/9780784480595.006.
Saksena, S., Merwade, V., Singhofen, P.J., 2019. Flood inundation modeling and mapping by integrating surface and subsurface hydrology with river hydrodynamics. J. Hydrol. 575, 1155–1177. https://doi.org/10.1016/j.jhydrol.2019.06.024.
Saksena, S., Dey, S., Merwade, V., Singhofen, P.J., 2020. A computationally efficient and physically based approach for urban flood modeling using a flexible spatiotemporal structure. Water Resour. Res. 56, e2019WR025769. https://doi.org/10.1029/2019WR025769.
Sampson, C.C., Fewtrell, T.J., Duncan, A., Shaad, K., Horritt, M.S., Bates, P.D., 2012. Use of terrestrial laser scanning data to drive decimetric resolution urban inundation models. Adv. Water Resour 41, 1–17. https://doi.org/10.1016/j.advwatres.2012.02.010.
Sampson, C.C., Smith, A.M., Bates, P.D., Neal, J.C., Alfieri, L., Freer, J.E., 2015. A high-resolution global flood hazard model. Water Resour. Res. 51, 7358–7381.
Savage, J.T.S., Bates, P.D., Freer, J.E., Neal, J.C., Aronica, G.T., 2016. When does spatial resolution become spurious in probabilistic flood inundation predictions? Hydrol. Proc. 30, 2014–2032. https://doi.org/10.1002/hyp.10749.
Schumann, G., Bates, P.D., Apel, H., Aronica, G.T., 2018. Global flood hazard mapping, modeling, and forecasting. Glob. Flood Haz. Geophys. Monogr. Ser. https://doi.org/10.1002/9781119217886.ch14.
Scott, D.T., Gomez-Velez, J.D., Jones, C.N., Harvey, J.W., 2019. Floodplain inundation spectrum across the United States. Nat. Commun. 10, 5194. https://doi.org/10.1038/s41467-019-13184-4.
Sibson, R., 1981. A Brief Description of Natural Neighbor Interpolation. John Wiley & Sons, New York, pp. 21–36.
Tapia-Silva, F.-O., Itzerott, S., Foerster, S., Kuhlmann, B., Kreibich, H., 2011. Estimation of flood losses to agricultural crops using remote sensing. Phys. Chem. Earth A/B/C 36, 253–265. https://doi.org/10.1016/j.pce.2011.03.005.
Tauro, F., Petroselli, A., Porfiri, M., Giandomenico, L., Bernardi, G., Mele, F., Spina, D., Grimaldi, S., 2016. A novel permanent gauge-cam station for surface-flow observations on the Tiber River. Geosci. Instrum. Methods Data Syst. 5, 241–251. https://doi.org/10.5194/gi-5-241-2016.
Teng, J., Vaze, J., Dutta, D., Marvanek, S., 2015. Rapid inundation modelling in large floodplains using LiDAR DEM. Water Resour. Manag. 29, 2619–2636. https://doi.org/10.1007/s11269-015-0960-8.
Tiber River Basin Authority, 2010. Piano Direttore dell'Autorità di Bacino del fiume Tevere (Flood Risk Management Plan) Rome (Italy).
Trigg, M.A., Wilson, M.D., Bates, P.D., Horritt, M.S., Alsdorf, D.E., Forsberg, B.R., Vega, M., 2009. Amazon flood wave hydraulics. J. Hydrol. 374, 92–105. https://doi.org/10.1016/j.jhydrol.2009.06.004.
Twilley, R.R., Bentley, S.J., Chen, Q., Edmonds, D.A., Hagen, S.C., Lam, N.S.-N., Willson, C.S., Xu, K., Braud, D., Hampton Peele, R., McCall, A., 2016. Co-evolution of wetland landscapes, flooding, and human settlement in the Mississippi River Delta Plain. Sustain. Sci. 11, 711–731. https://doi.org/10.1007/s11625-016-0374-4.
UNISDR, 2015. The Human Cost of Weather Related Disasters, CRED 1995–2015 Geneva, Switzerland.
Valentová, J., Valenta, P., Weyskrabová, L., 2010. Assessing the retention capacity of a floodplain using a 2D numerical model. J. Hydrol. Hydromech. 58, 221–232. https://doi.org/10.2478/v10098-010-0021-1.
Veja-Serratos, B.E., Dominguezz-Mora, R., Posada-Vanegas, G., 2018. Seasonal flood risk assessment in agricultural areas. Tecnol. Cienc. Agua 9, 92–127.
Vozinaki, A.-E.K., Karatzas, G.P., Sibetheros, I.A., Varouchakis, E.A., 2015. An agricultural flash flood loss estimation methodology: the case study of the Koiliaris basin (Greece), February 2003 flood. Nat. Hazards 79, 899–920. https://doi.org/10.1007/s11069-015-1882-8.
Ward, P.J., Jongman, B., Salamon, P., Simpson, A., Bates, P.D., De Groeve, T., Muis, S., De Perez, E.C., Rudari, R., Trigg, M.A., Winsemius, H.C., 2015. Usefulness and limitations of global flood risk models. Nat. Clim. Chang. 5, 712–715. https://doi.org/10.1038/nclimate2742.
Wing, O.E.J., Bates, P.D., Sampson, C.C., Smith, A.M., Johnson, K.A., Erickson, T.A., 2017. Validation of a 30 m resolution flood hazard model of the conterminous United States. Water Resour. Res. 53, 7968–7986. https://doi.org/10.1002/2017WR020917.
Wing, O.E.J., Pinter, N., Bates, P.D., Kousky, C., 2020. New insights into US flood vulnerability revealed from flood insurance big data. Nat. Commun. 11, 1444. https://doi.org/10.1038/s41467-020-15264-2.
Winsemius, H.C., Van Beek, L.P.H., Jongman, B., Ward, P.J., Bouwman, A., 2013. A framework for global river flood risk assessments. Hydrol. Earth Syst. Sci. 17, 1871–1892. https://doi.org/10.5194/hess-17-1871-2013.
Yamazaki, D., O'Loughlin, F., Trigg, M.A., Miller, Z.F., Pavelsky, T.M., Bates, P.D., 2014. Development of the global width database for large rivers. Water Resour. Res. 1, 3467–3480. https://doi.org/10.1002/2013WR014664.Received.
Yu, D., Lane, S.N., 2011. Interactions between subgrid-scale resolution, feature representation and grid-scale resolution in flood inundation modelling. Hydrol. Process. 25, 36–53. https://doi.org/10.1002/hyp.7813.